https://dx.doi.org/10.1016/j.jcsr.2019.105711

Buckling resistance of welded high-strength-steel box-section members under combined compression and bending

Han Fang[a,*] and Tak-Ming Chan[b]

[a]School of Civil, Environmental and Mining Engineering, The University of Adelaide, South Australia 5005, Australia

[b]Department of Civil and Environmental Engineering, The Hong Kong Polytechnic University, Hong Kong, China

*han.fang@adelaide.edu.au

Abstract

The global buckling resistance of welded high strength steel box section members subject to combined compression and bending was investigated through a numerical modelling programme. Finite element models were developed with the capability to accurately replicate the experimental results of the box section members under combined compression and bending. Extensive parametric studies were carried out to examine the global buckling behaviour of welded high strength steel box section members with a wide range of dimensions and member slenderness and steel grades of S460, S690 and S960 and subject to varying combinations of compression and bending. The effects of residual stresses and ultimate tensile strength-to-yield strength ratio on the global buckling behaviour of those members were investigated. The applicability of existing design rules to welded high strength steel box section members subject to combined compression and bending was evaluated using the results from parametric studies and the available experimental results in literature. The European, American and Australian standards provide conservative strength predictions for the structures. More accurate and safe strength predictions can be obtained based on European standard using the suggested column curves for the members while the design methods in Australian and American standards are safely applicable to the members.

Keywords: High strength steel, welded box section member, combined compression and bending, finite element modelling, design

1. Introduction

High strength steel (HSS) with yield strength over 460MPa has been increasingly applied in structural applications such as roof trusses and bridges [1-2]. By using high strength steel, structural elements with smaller sizes than conventional strength steel structures can be selected for structural designs. Consequently, the saving of weight consumption of construction materials can be achieved and subsequently brings advantages such as savings of transportation costs and easier handling during construction. Extensive research studies have been carried out to characterise the behaviour of welded HSS structures in order to conduct accurate structural designs. Residual stresses of welded HSS box and I-sections were measured [3-6]. Experimental and numerical investigations were also performed to examine the behaviour of the welded HSS structures subject to axial compression [7-11] or bending [12-14] and design approaches have been proposed based on these experimental and numerical investigations [13, 15-16]. Despite these systematic research studies on welded HSS structures subject to axial compression or bending, the behaviour of these structures subject to combined compression and bending also needs to be clearly understood in order to obtain accurate structural designs for the combined loading conditions but has received much less attention.

Nie and the co-workers [17] conducted experimental and numerical investigations on welded Q460GJ steel box section members under combined compression and bending. The experimental and numerical results were compared with the design strength predictions from different standards. It was found in the study that European and Chinese standards provided conservative strength predictions for the structures while American and Japanese standards provided quite accurate strength predictions. Experiments were also conducted to investigate welded box section members with the nominal yield strength of 690MPa and subject to combined compression and bending [18-19]. In addition, Ban and the co-workers [10] investigated the welded HSS box section members with nominal yield strength of 960MPa and tested two members under combined compression and bending. The review of the aforementioned studies on welded HSS box section members under combined compression and bending reveal that each study only covers the members with one specific steel grade and limited dimensions. No systematic studies have been carried out to examine the behaviour of welded HSS box section members with different steel grades and subject to different combinations of compression and bending. In addition, current standards including European, American and Australian standards [20-22] provide design methods for members with the steel grade up to S700. The applicability of the design methods in standards for these structures with varying steel grades up to S960 is unknown and needs to be accurately evaluated in order to achieve safe and economical structural designs.

Therefore, in this study, the global buckling behaviour of welded HSS box section members with steel grades of S460, S690 and S960 and subject to combined compression and bending was investigated

numerically. FE models were developed and validated using the experimental results of welded HSS box members under combined compression and bending. Subsequently, extensive parametric studies were performed. The applicability of design rules in European, American and Australian standards for the members under combined compression and bending was evaluated using the results of parametric studies conducted in this study and experiments reported in literature.

2. Finite element modelling

A numerical investigation into the global buckling resistance of welded HSS box section members subject to combined compression and bending was carried out using the non-linear finite element analysis package ABAQUS [23]. Finite element (FE) models were developed to replicate the experimental results for welded box section members with steel grades of S460, S690 and S960 and subject to combined compression and bending [10, 17-19]. The experimental results are summarised in Table 1. In the table, the labels for the members are based on the member cross-sectional dimensions. For each label, the letter "B" indicates the box section members while the following digits represent the width of the cross-section and plate thickness. The validated FE models were employed to conduct parametric studies to expand the structural performance database covering a wide range of cross-sectional dimensions, member slenderness values, steel grades and combinations of loading.

2.1 Development of the finite element models

The four-noded S4R shell element with reduced integration was applied to simulate the behaviour of welded HSS box section members. The mesh size of plate thickness was selected for box section members to obtain accurate estimations of the structural performance. The stress-strain relationship of HSS was simulated using multi-linear stress-strain models. The model adopted for S460 steel is presented in Fig. 1(a) considering the yield plateau observed in the measured stress-strain curves for the material [7, 17]. The model presented in Fig. 1(b) was suggested for S690 and S960 steel [16] and adopted in this study. The values for material property parameters highlighted in Fig. 1 are based on the measurements of material properties for the welded HSS box section members tested under combined compression and bending [10, 17-19]. The stress-strain curves obtained using the models were converted into true stress-logarithmic plastic strain curves which were subsequently incorporated into the FE models.

Residual stresses exist in the welded box section members with steel grades of S460, S690 and S960 due to the welding fabrication. Residual stress models for these members were provided by Shi et al. [8] and the residual stresses estimated using the models were applied to obtain accurate FE modelling results for the members under axial compression [16]. Based on these residual stress models, the

magnitudes and pattern of residual stresses were obtained for the current investigation and included as initial stresses for the FE models of welded box section members with steel grades of S460, S690 and S960 and subject to combined compression and bending.

The boundary conditions were defined in the FE models to simulate the pin-supported conditions applied to the members in experiments [10, 17-19]. Two eccentric reference points were created and each reference point was coupled with one end section of a member. The reference points were offset from the buckling axis through the centroid of the member by the loading eccentricity (e). The longitudinal distance between the reference points equal to the effective length (L_{eff}) of any member. All degrees of freedom were restrained at the reference point on the unloaded side, except for the rotations about the buckling axis. The same boundary conditions were also applied to the reference point on the loaded side except that the longitudinal displacement was allowed. The loading was applied in a Riks step at the reference point on the loaded side by specifying a displacement rate in the longitudinal direction. The modified Riks method was employed to trace the load-deformation behaviour of the welded HSS box section members.

Initial geometric imperfections in the welded HSS box section members can influence the structural performance of the members [16] and were also taken into account in the FE models. Prior to the analysis using the Riks step, an elastic eigenvalue analysis was conducted for each member. The resultant lowest elastic global buckling mode shape was adopted as the global geometric imperfection pattern and subsequently incorporated into the FE models with the amplitudes of the global geometric imperfection measured for the members in Table 1 [10, 17-19]. Since the cross-sections of the members investigated in the current study are Class 1-3 sections based on the European standard [22], the effect of local geometric imperfections would be quite limited. Thus, no local geometric imperfection was incorporated in the FE models.

2.2 Validation

The FE models were validated through comparing the FE results with the experimental results of welded HSS box section members subject to combined compression and bending. The comparison of ultimate loads ($P_{u,FE}$) estimated using the FE models with those from experiments (P_{exp}) is shown in Table 1. It is observed from the table that the ultimate loads were accurately estimated. The mean value of $P_{u,FE}/P_{exp}$ ratios was found to be 1.00 with the coefficient of variation (COV) of 0.02. The load and displacement responses estimated in FE modelling for the members were also compared with those obtained from experiments. Typical load versus mid deflection curves for welded box section members under compression and bending are presented in Fig. 2. As can be seen in the figures, the curves from FE modelling compared well with those from experiments. Excellent agreement between the global buckling failure mode observed for the members tested in experiments and that predicted in

FE modelling was also obtained, as shown in Figs. 3 and 4. The comparison between the results from experiments and FE modelling reveals that the FE models are capable of accurately replicating the experimental results and validated for performing parametric studies.

3. Parametric studies

3.1 General

Having the FE models validated, parametric studies were carried out on the welded S460, S690 and S960 steel box section members with a wide range of cross-sectional dimensions and member slenderness and subject to various combinations of compression and bending. Effects of residual stresses and material tensile-to-yield strength ratio on the global buckling behaviour of these members subject to combined compression and bending were evaluated. These parameters and their values are presented in Table 2. The cross-sectional dimensions for parametric studies were based on those for specimens tested in experiments, covering the Class 1-3 cross-sections according to the cross-sectional classification specifications in European standard [22]. The length of the members varies to obtain the member slenderness values between 0.3 and 2.5 according to European standard. Initial geometric imperfections were also incorporated in the modelling for the welded HSS box section members and the magnitude suggested as 1/1000 of the member length [10, 17, 24] was adopted. Different combinations of compression and bending were achieved by varying e. The values for e were selected in relation to the cross-section dimensions and the initial loading eccentricity ratio (ε_r) which was defined in Eq. (1). In the equation, A is the cross-sectional area while W is the elastic modulus of the cross-section. The ε_r values from 0 to 6.0 were selected for parametric studies.

$$\varepsilon_r = \frac{eA}{W} \tag{1}$$

The residual stress pattern and magnitudes estimated using the models from Shi et al. [8] were also adopted for the parametric studies. The effect of residual stresses on the global buckling behaviour of welded HSS box section members subject to combined compression and bending was also investigated using the members with the B168*12 section. The modelling results for the members with and without the incorporation of residual stresses were compared, as presented in Section 3.2. Material stress-strain relationship for the parametric studies were obtained using the models given in Fig. 1 and based on the average measured material properties in the experimental investigations [10, 17-19], as shown in Table 3. The measurement results for the material properties in the experimental investigations into welded HSS box section members subject to combined compression and bending [10, 17, 19] also show that the material tensile-to-yield strength ratio (f_u/f_y) varies for the material in each steel grade. Therefore, the effect of f_u/f_y ratio was also quantified using members with the B168*12 section, as presented in Section 3.3.

3.2 Effect of residual stresses

The effect of residual stresses was investigated based on the B168*12 section members with varying member slenderness values and subject to combined compression and bending. The residual stresses in welded HSS box section members are in equilibrium and their distribution across the box cross-sections is approximately symmetric [3, 5, 8]. The global buckling behaviour for the members with and without the input of residual stresses were investigated. The resultant ultimate loads ($P_{u,FE}$) normalised by the cross-sectional capacity as $A*f_y$ are plotted against member slenderness values, as shown in Fig. 5 for S460, S690 and S960 members. As can be seen in the figures, the $P_{u,FE}/A*f_y$ are dependent on the residual stresses and the decreasing effect of residual stresses decreases with increasing initial eccentricity ratio for members with the same member slenderness value and steel grade. The residual stresses led to a maximum reduction of about 20, 18 and 14% of the $P_{u,FE}/A*f_y$ for S460, S690 and S960 members respectively when the loading eccentricity is zero. With increasing loading eccentricity ratio from zero to 0.67, the maximum reduction of $P_{u,FE}/A*f_y$ due to the incorporation of residual stresses decreased to be about 6.2, 5.6 and 2.4% for S460, S690 and S960 members respectively. For higher loading eccentricity ratios equal to 2 and 4, the decrement of $P_{u,FE}/A*f_y$ due to residual stresses is below 5.0, 3.5 and 2.1 % for S460, S690 and S960 members respectively. For the members subject to compression with ε_r value of zero, the combined compressive stresses due to external compressive loading and compressive residual stresses can lead to early yielding at certain locations of the members, resulting in the reduction of their ultimate loads. For the members subject to bending moment, tensile and compressive stresses due to the bending moment are in equilibrium within the box cross-sections. Therefore, the effect of residual stresses on the ultimate strengths of members subject to bending can be relatively limited. With increasing ε_r values, the bending moment exerted on the members increases. Therefore, the ultimate strengths of members with ε_r values above zero are less sensitive to residual stresses. Besides, the decreasing effect of residual stresses on the global buckling resistances is also related to the member slenderness value. The decreasing effect is larger for members with member slenderness values between 0.7 and 1.1, as shown in Fig. 5.

3.3 Effect of f_u/f_y ratio

The effect of tensile-to-yield strength (f_u/f_y) ratio on the global buckling behaviour of welded box section members in steel grades of S460, S690 and S960 was also investigated based on the B168*12 section members with varying member slenderness values and subject to combined compression and bending. The $P_{u,FE}$ for the members were estimated based on the lower and upper limits of f_u/f_y ratio by varying ultimate tensile strength of the material in each steel grade. The lower and upper limits of f_u/f_y ratio for the investigation were determined according to the EN10025-6 standard [25] for high

196 strength steel products and are provided in Table 3. The $P_{u,FE}$ obtained using the lower and upper
197 limits of f_u/f_y ratio are normalised by $A*f_y$ and plotted against member slenderness values in Fig. 6 for
198 S460, S690 and S960 members. As can be seen in the figures, the effect of f_u/f_y ratio is observed for
199 the members with low slenderness values since the maximum strains reached in these members at
200 their ultimate loads are greater than the material yield strains. Thus, the ultimate loads of these
201 members are affected by the material strain hardening behaviour.

202 For welded S460 box section members with the lowest slenderness value of 0.3, the $P_{u,FE}/A*f_y$
203 obtained based on the upper limit of f_u/f_y ratio is larger than the $P_{u,FE}/A*f_y$ based on the lower f_u/f_y
204 ratio by about 10, 0.5, 0.9 and 0.5% when the ε_r equals to 0, 0.67, 2, 4 respectively. For the welded
205 S460 box section members with larger slenderness values, no effect of f_u/f_y ratio on the $P_{u,FE}/A*f_y$ is
206 observed since there is a yield plateau in the stress-strain relationship of S460 steel and the strains
207 obtained when the structures fail are below the strain (ε_{sh}) representing the largest strain in the yield
208 plateau. As for the welded S690 and S960 box section members, the effect of f_u/f_y ratio is the largest
209 when the member slenderness value is 0.3 and the $P_{u,FE}/A*f_y$ increases by 3-7% based on the upper
210 limit of f_u/f_y ratio. The effect decreases with increasing member slenderness up to 1.1 while minimal
211 effect of f_u/f_y ratio can be observed for the welded S690 and S960 box section members with member
212 slenderness above 1.1.

213 # 4. Assessment of existing design rules and design recommendations

214 The applicability of existing design rules in European, American and Australian standards to the
215 welded box section members with steel grades from S460 to S960 and subject to combined
216 compression and bending was evaluated. The results of ultimate loads (P_u) from the parametric studies
217 introduced in Section 3 and experiments reported in literature were compared with the unfactored
218 strength predictions (P_d) based on the design rules. The accuracy of existing design rules for those
219 members was discussed. In addition, the applicability of alternative column curves suggested in
220 literature [16, 26] for the members has also been evaluated.

221 ## 4.1 European code EN1993-1-1

222 European code EN1993-1-1 [22] provides interaction formulae given as Eqs. (2) and (3) for members
223 subject to combined compression and bending. In these equations, P_c is the member resistance in axial
224 compression, M_c is the member resistance in bending, P_d is the design axial load, M_d is the design
225 bending moment and taken as the end moment (M_{end}), and k_{yy}, k_{yz}, k_{zy} and k_{zz} are the interaction
226 factors. According to EN1993-1-1, P_c values can be estimated based on column buckling curves
227 giving the variation of normalised member resistance in compression with the member slenderness
228 and the column buckling curve c is specified for welded box section members. For calculating the

interaction factors, two approaches are provided in Annexes A and B and used for predicting the P_d in this study.

$$\frac{P_d}{P_c} + k_{yy}\frac{M_{d,y}}{M_{c,y}} + k_{yz}\frac{M_{d,z}}{M_{c,z}} \leq 1 \quad (2)$$

$$\frac{P_d}{P_c} + k_{zy}\frac{M_{d,y}}{M_{c,y}} + k_{zz}\frac{M_{d,z}}{M_{c,z}} \leq 1 \quad (3)$$

The $P_{d,EC3}$ predicted based on Annexes A and B are compared with the results from FE modelling and experiments ($P_{u,exp+FE}$) for welded HSS box section members in Figs. 7 and 8 respectively, where the $P_{u,exp+FE}/P_{d,EC3}$ ratios are plotted against the parameter θ describing the combinations of compression and bending [28] and taken as $\tan^{-1}\left(\frac{P/P_c}{M/M_c}\right)$. As can be seen in Figs. 7 and 8, the European code provides conservative strength predictions for the members. The mean $P_{u,FE+exp}/P_{d,EC3}$ ratios based on Annex A for the members are 1.09-1.12 with COV of 0.05-0.06 while the mean $P_{u,FE+exp}/P_{d,EC}$ ratios based on Annex B are 1.11-1.14 with COV of 0.04-0.06, as summarised in Tables 4-6 for S460, S690 and S960 members respectively. In order to improve the accuracy of strength predictions based on EN1993-1-1, the column buckling curve b was suggested for welded S460 and S690 members while column buckling curve a was suggested for welded S960 members [16, 26]. The applicability of these curves to welded S460, S690 and S960 members subject to combined compression and bending was assessed. The $P_{d,EC3}$ values estimated based on curves b and a for the members are compared with the ultimate loads from the FE parametric studies and experiments reported in literature, as shown in Figs. 7 and 8 and Tables 4-6. As can be seen in the figures and tables, the accuracy of strength predictions for welded S460 and S690 members is improved by using column buckling curve b. Comparing with the strength predictions based on column buckling curve c for welded S960 members, the strength predictions obtained using the column buckling curve a agree better with the results from parametric studies and experiments reported in literature and are safe-sided on an average basis.

4.2 AISC 360

The AISC 360 standard [20] provides two interaction formulae for structural members bending about a single axis under combined compression and bending, as given as Eqs. (4) and (5). The P_c was estimated using the single column curve specified in Chapter E of AISC 360 standard while the M_c was estimated in accordance with the specifications in Chapter F of the standard. M_d was calculated as the end moment (M_{end}) multiplied by $1/(1-P_d/P_{cr})$.

$$\frac{P_d}{P_c} + \frac{8}{9}\frac{M_d}{M_c} \leq 1 \ \ for \ \frac{P_d}{P_c} \geq 0.2 \quad (4)$$

$$\frac{P_d}{2P_c} + \frac{M_d}{M_c} \leq 1 \ for \frac{P_d}{P_c} < 0.2 \quad (5)$$

The results from the parametric studies and experiments reported in literature for the welded HSS S460, S690 and S960 box section members are compared with the strength predictions based on Eqs. (4) and (5), as shown in Fig. 9. It can be seen in the figures that the data points are mostly above the curve representing that the $P_{u,exp+FE}/P_{d,AISC}$ ratio equal to unity. The mean values of $P_{u,FE+exp}/P_{d,AISC}$ ratios for welded box section members in S460, S690 and S960 were also calculated and found to be 1.03, 1.06 and 1.06 respectively with the corresponding COV of 0.06, 0.05 and 0.05, as given in Tables 4-6. The comparison shows that the strength predictions based on AISC 360 standard are conservative on an average basis.

4.3 AS4100

In AS4100 Australian standard [21], a linear interaction formula given as Eq. (6) is provided for any member subject to combined compression and bending about a principle axis. For the estimation of P_c, five column curves related to different values of member section constant (α_b) are provided in Clause 6.3 of AS4100 standard. The column curve based on the α_b value of zero can be applied to welded S460 box section members while the column curve based on the α_b value of -0.5 is specified for welded S690 box section members. For S960 members, no specification for the column curve is provided and the applicability of the curve based on the α_b value of -0.5 was assessed. The M_c was calculated according to the specifications in Clause 5.2 of AS4100 standard. M_d is also taken as the end moment (M_{end}) multiplied by $1/(1-P_d/P_{cr})$, in which P_{cr} is the elastic buckling load.

$$\frac{P_d}{P_c} + \frac{M_d}{M_c} \leq 1 \tag{6}$$

The ratios of ultimate loads from parametric studies presented in Section 3 and experiments reported in literature over P_d estimated using Eq. (6) for the welded HSS S460, S690 and S960 box section members are plotted against the θ values in Fig. 10. The comparison of FE and experimental results with the strength predictions in Fig. 10 shows that the strength predictions based on AS4100 are conservative for welded S460, S690 and S960 box section members. The mean values of $P_{u,FE+exp}/P_{d,AS}$ ratios for the welded S460, S690 and S960 box section members respectively were also calculated to be about 1.09, 1.11 and 1.10 with the COV of 0.07, 0.05 and 0.05, as given in Tables 4-6. Therefore, AS4100 standard provide conservative strength predictions for the structures.

4.4 Reliability analysis

Reliability analysis was also conducted to examine the reliability of the aforementioned design methods for welded HSS box section members according to EN1990 standard [29] and AISC 360 standard [20]. The analysis was separately conducted for members with ε_r of zero and those with ε_r greater than zero, based on the parametric studies results in this study and experimental results in

literature for welded HSS box section members subject to compression and combined compression and bending [7, 9, 10, 17-19, 26-27]. In the assessment, the values of mean to nominal yield strength ratio and the COV of the material yield strength (V_f) for S460 and S690 steel are based on those given by Wang et al. [30]. For S960 steel, the mean to nominal yield strength ratio and V_f were estimated to be 1.059 and 0.0415 respectively based on the collected results of material properties measurements conducted by researchers [6, 10, 26, 31-42] and the Ruukki steel producer. The value of COV for the geometric properties (V_g) was taken as 0.02 according to Wang et al. [30] and Byfield and Nethercot [43]. For the reliability analysis in accordance with EN1990 standard [29] for the design method given in European code EN1993-1-1, the key parameters are given in Table 7, where n is the number of tests and FE results, $k_{d,n}$ is the design fractile factor, b_e is the average ratio of experiment or FE to design model resistance based on a least-squares fit to all the data, V_δ is the COV of tests and FE results relative to the design strengths, V_r is the combined coefficient of variation incorporating both design model and basic variable uncertainties and γ_{M1} is the required partial safety factor applied to the denominator for predicting the strengths of the structures. The γ_{M1} values calculated to satisfy the requirement for the target reliability index (β) value of 3.8 are also given in Table 7. As can be seen in the table, the γ_{M1} values obtained based on the column curve c for S460 steel members are between 0.95 and 0.99 while the γ_{M1} values obtained based on the column curve b for the members are about 1.01-1.03 and larger than the value of 1.0 specified for γ_{M1} in European code EN1993-1-1. For the S690 members, the γ_{M1} values obtained based on the column curve c and b are between 0.91 and 0.99. As for the S960 members, the γ_{M1} values obtained based on the column curve c are about 0.96-0.97 while the γ_{M1} values obtained based on the column curve a are about 1.04-1.05. From these results, a higher value of 1.05 for γ_{M1} is recommended especially for the application of curve b for S460 members and curve a for S960 members.

The reliability analysis for the design method in AISC 360 was also conducted in accordance with the specifications given by the standard. The load combination of 1.2×dead load+1.6×live load and the dead-to-live load ratio of 1/3 were adopted for the analysis. Table 8 presents the key parameters including V_Q as the COV of the load effects, V_R as the COV of resistance and ϕ as the safety factor with the value of 0.9 in AISC 360 standard being applied to the numerator for strength predictions. Based on these parameters, β values were calculated for the welded box section members in different steel grades and subject to compression with ε_r value of zero or combined compression and bending with ε_r values greater than zero and are also presented in Table 8. It can be seen in the table, the β values vary between 2.89 and 3.33 and are larger than the target value of 2.6. Therefore, the design method in AISC 360 standard can be safely applied. Since the design method in AS4100 provides more conservative strength predictions than the methods from European code EN1993-1-1 or AISC

360 and specifies the safety factor value of 0.9 applied to the numerator for strength predictions, the AS4100 design method can be considered to be satisfactory with acceptable reliability.

5. Conclusions

A systematic numerical investigation into the global buckling resistance of welded HSS box section members subject to combined compression and bending was conducted. FE models were developed and validated to be capable of accurately replicating the results of experiments on the members in steel grades between S460 and S960 and subject to combined compression and bending. Subsequent parametric studies were carried out, covering a wide range of cross-sectional and member slenderness and various combinations of compression and bending for the welded S460, S690 and S960 box section members. Effect of residual stresses was investigated and the decreasing effect on the ultimate loads of the members was found to reduce with increasing eccentricity ratio. Besides, the decreasing effect of residual stresses was also observed to be larger for members with member slenderness values between 0.7 and 1.1. Effect of tensile-to-yield strength (f_u/f_y) ratio was also investigated and was observed for the S460, S690 and S960 members with relatively lower member slenderness.

The applicability of design methods in European, American and Australian standards to welded box section members with steel grades of S460, S690 and S960 and subject to combined compression and bending was also assessed using the parametric studies results in this study and experimental results reported in literature. Based on these design methods, the ultimate loads of the members were underestimated by about 3-14%. The accuracy of strength predictions based on suggested column curves from Ban and Shi [16] and Somodi and Kövesdi [26] for European standard EN1993-1-1 was also evaluated. The evaluation reveals that the strength predictions based on the suggested column curves from Ban and Shi [16] and Somodi and Kövesdi [26] are also conservative and more accurate than the predictions based on the original design method in European standard EN1993-1-1. Reliability of these design methods was examined through reliability analysis which shows that the design method in European standard with a partial safety factor value of 1.05 and the methods in AS4100 and AISC 360 standards can be applied to welded S460, S690 and S960 box section members subject to combined compression and bending.

Acknowledgement

The authors are grateful for the support from the Chinese National Engineering Research Centre for Steel Construction (Hong Kong Branch) at The Hong Kong Polytechnic University. The financial support from The Hong Kong Polytechnic University (PolyU: 1-ZE50/GYBUU) is also gratefully acknowledged.

References

[1] Ma, J.L., Chan, T.M. and Young, B. 2015. Material properties and residual stresses of cold-formed high strength steel hollow sections. *Journal of Constructional Steel Research*, 109, 152-165.

[2] Gkantou, M. 2017. Response and design of high strength steel structures employing square and rectangular hollow sections. Ph.D. thesis. Department of Civil Engineering, University of Birmingham.

[3] Ban, H.Y., Shi, G., Shi, Y.J. and Wang, Y.Q. 2013. Residual stress of 460 MPa high strength steel welded box section: Experimental investigation and modeling. *Thin-Walled Structures*, 64, 73-82.

[4] Ban, H.Y., Shi, G., Shi, Y.J. and Wang, Y.Q. 2013. Residual stress of 460 MPa high strength steel welded I section: Experimental investigation and modeling. *International Journal of Steel Structures*, 13, 691-705.

[5] Li, T.J., Li, G.Q. and Wang, Y.B. 2015. Residual stress tests of welded Q690 high-strength steel box- and H-sections. *Journal of Constructional Steel Research*, 115, 283-289.

[6] Shi, G., Zhou, W.J. and Lin, C.C. 2015. Experimental investigation on the local buckling behaviour of 960 MPa high strength steel welded section stub columns. *Advances in Structural Engineering*, 18, 423-437.

[7] Ban, H.Y., Shi, G., Shi, Y.J. and Wang, Y.Q. 2012. Overall buckling behaviour of 460 MPa high strength steel columns: Experimental investigation and design method. *Journal of Constructional Steel Research*, 74, 140-150.

[8] Shi, G., Xu, K.L., Ban, H.Y. and Lin, C.C. 2016. Local buckling behaviour of welded stub columns with normal and high strength steels. *Journal of Constructional Steel Research*, 119, 144-153.

[9] Li, T.J., Li, G.Q., Chan, S.L. and Wang, Y.B. 2016. Behavior of Q690 high-strength steel columns: Part 1: Experimental investigation. *Journal of Constructional Steel Research*, 115, 283-289.

[10] Ban, H.Y., Shi, G., Shi, Y.J. and Bradford, M.A. 2013. Experimental investigation of the overall buckling behaviour of 960MPa high strength steel columns. *Journal of Constructional Steel Research*, 88, 256-266.

[11] Fang, H. and Chan, T.M. 2018. Axial compressive strength of welded S460 steel columns at elevated temperatures. *Thin-walled Structures*, 129, 213-224.

[12] Lee, C.H., Han, K.H., Uang, C.M., Kim, D.K., Park, C.H. and Kim, J.H. 2013. Flexural strength and rotation capacity of I-shaped beams fabricated from 800-MPa Steel. *Journal of Structural Engineering*, 139, 1043-1058.

[13] Shokouhian, M. and Shi, Y.J. 2015. Flexural strength of hybrid I-beams based on slenderness. *Engineering Structures*, 93, 114-128.

391 [14] Shi, Y.J., Xu, K.L., Shi, G. and Li, Y.X. 2017. Local buckling behavior of high strength steel
392 welded I-section flexural members under uniform moment. *Advances in Structural Engineering*, 00,
393 1-16.
394 [15] Chan, T.M., Zhao, X.L. and Young, B. 2015. Cross-section classification for cold-formed and
395 built-up high strength carbon and stainless steel tubes under compression. *Journal of Constructional*
396 *Steel Research*, 106, 289-295.
397 [16] Ban, H.Y. and Shi, G. 2018. Overall buckling behaviour and design of high-strength steel welded
398 section columns. *Journal of Constructional Steel Research*, 143, 180-195.
399 [17] Nie, S.D., Kang, S.B., Shen, L. and Yang, B. 2017. Experimental and numerical study on global
400 buckling of Q460GJ steel box columns under eccentric compression. *Engineering Structures*, 142,
401 211-222.
402 [18] Usami, T. and Fukumoto, Y. 1982. Local and overall buckling of welded box columns. *Journal*
403 *of the Structural Division*, 108, 525-542.
404 [19] Rasmussen, K.J.R. and Hancock, G.J. 1995. Tests of High Strength Steel Columns. *Journal of*
405 *Constructional Steel Research*, 34, 27-52.
406 [20] ANSI/AISC 360-16, 2016. *Specification for structural steel buildings*. AISC, Chicago.
407 [21] AS4100, 1998. *Australian Standard. Steel structures.* NSW, Australia: Standards Australia.
408 [22] EN 1993-1-1:2005+A1, 2014. *Eurocode 3: Design of steel structures - Part 1-1: General rules*
409 *and rules for buildings*. Brussels: European Committee for Standardization.
410 [23] ABAQUS [Computer software] (2012). Dassault Systèmes, Providence, RI.
411 [24] Ma, T.Y., Li, G.Q. and Chung, K.F. 2018. Numerical investigation into high strength Q690 steel
412 columns of welded H-sections under combined compression and bending. *Journal of Constructional*
413 *Steel Research*, 144, 119-134.
414 [25] EN 10025-6, 2004+A1: 2009. *Hot rolled products of structural steels - Part 6: Technical*
415 *delivery conditions for flat products of high yield strength structural steels in the quenched and*
416 *tempered condition*. Brussels: European Committee for Standardization.
417 [26] Somodi, B. and Kövesdi, B. 2017. Flexural buckling resistance of welded HSS box section
418 members. *Thin-Walled Structures*, 119, 266-281.
419 [27] Kövesdi, B. and Somodi, B. 2018. Comparison of safety factor evaluation methods for flexural
420 buckling of HSS welded box section columns. *Structures*, 15, 43-55.
421 [28] Bu, Y.D. and Gardner, L. 2019. Laser-welded stainless steel I-section beam-columns: Testing,
422 simulation and design. *Engineering Structures*, 179, 23-36.
423 [29] EN 1990, 2002. "Eurocode – Basis of structural design." CEN, Brussels, Belgium.
424 [30] Wang, J., Afshan, S., Gkantou, M., Theofanous, M., Baniotopoulos, C. and Gardner, L. 2016.
425 Flexural behavior of hot-finished high strength steel square and rectangular hollow sections. *Journal*
426 *of Constructional Steel Research*, 121, 97-109.

[31] Shi, G., Ban, H.Y. and Bijlaard, F.S.K. 2012. Tests and numerical study of ultra-high strength steel columns with end restraints. *Journal of Constructional Steel Research*, 70, 236-247.

[32] Somodi, B. and Kövesdi, B. 2017. Flexural buckling resistance of cold-formed HSS hollow section members. *Journal of Constructional Steel Research*, 128, 179-192.

[33] Qiang, X.H., Jiang, X., Bijlaard, F.S.K. and Kolstein, H. 2016. Mechanical properties and design recommendations of very high strength steel S960 in fire. *Engineering Structures*, 112, 60-70.

[34] Guo, W., Crowther, D., Francis, J.A. Thompson, A., Liu, Z. and Li, L. 2015. Microstructure and mechanical properties of laser welded S960 high strength steel. *Materials and Design*, 85, 534-548.

[35] Akihide, N., Takayuki, I. and Tadashi, O. 2008. *Development of YP 960 and 1100MPa class ultra high strength steel plates with excellent toughness and high resistance to delayed fracture for construction and industry machinery*. JFE Technical report, no.11.

[36] Ślęzak, T. and Śnieżek, L. 2015. A comparative LCF study of S960QL high strength steel and S355J2 mild steel. *Procedia Engineering*, 114, 78-85.

[37] Gáspár, M. and Sisodia, R. 2018. Improving the HAZ of Q+T high strength steels by post weld heat treatment. *IOP Conference Series: Material Science and Engineering*, 426, 012012.

[38] Garašić, I., Ćorić, A., Kožuh, Z. and Samardžić, I. 2010. Occurrence of cold-cracks in welding of high-strength S960QL steel. *Technical Gazatte*, 17, 327-335.

[39] Coelho, A.M.G., Bijlaard, F.S.K. and Kolstein, H. 2009. Experimental behaviour of high-strength steel web shear panels. *Engineering Structures*, 31, 1543-1555.

[40] Dowding, R.G., Pinna, C., Ghadbeigi, H. and Farrugia, D. 2018. Localised damage analysis for high strength S960 steel using micro-tensile testing and digital image correction. *Ubiguity Proceedings*, 1, 16.

[41] Amraei, M., Dabiri, M., Björk, T. and Skriko, T. 2016. Effects of workshop fabrication processes on the deformation capacity of S960 ultra-high strength steel. *Journal of Manufacturing Science and Engineering*, 138, 121007 1-13.

[42] Neimitz, A., Dzioba, I. and Limnell, T. 2012. Modified master curve of ultra high strength steel. *International Journal of Pressure Vessels and Piping*, 92, 19-26.

[43] Byfield, M.P. and Nethercot, D.A. 1997. Material and geometric properties of structural steel for use in design. *The Structural Engineer*, 75, 363-367.

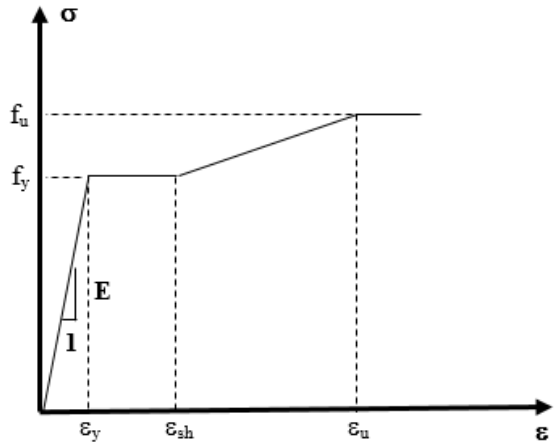

(a)

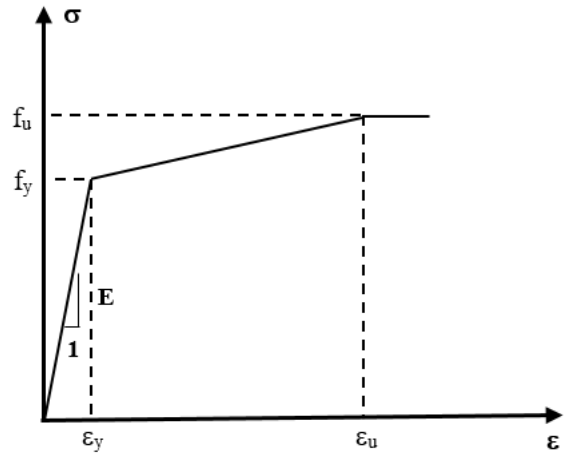

(b)

Figure 1. Stress-strain models for (a) S460 and (b) S690 and S960 high strength steel.

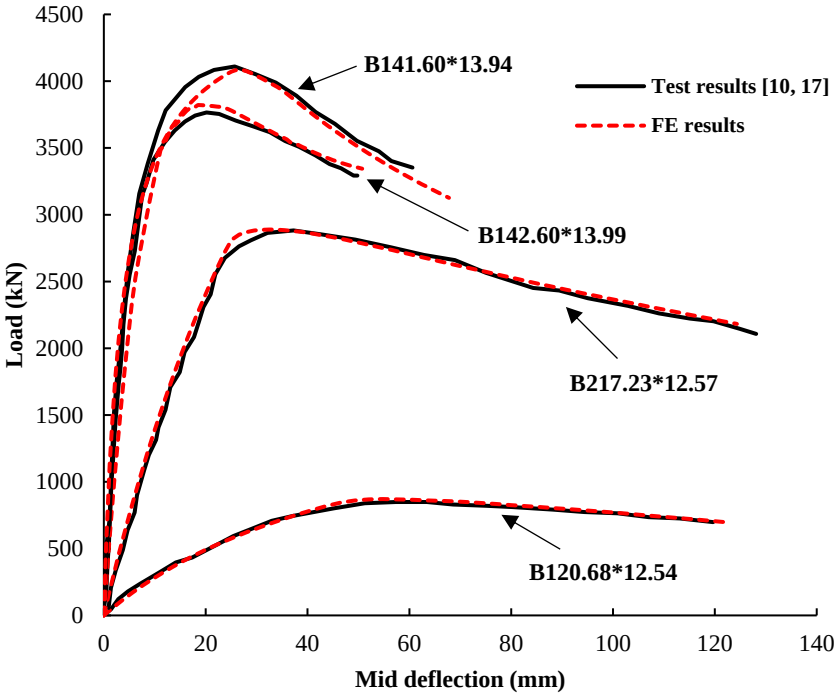

Figure 2. Comparison of load-mid deflection curves obtained from FE modelling and experiments.

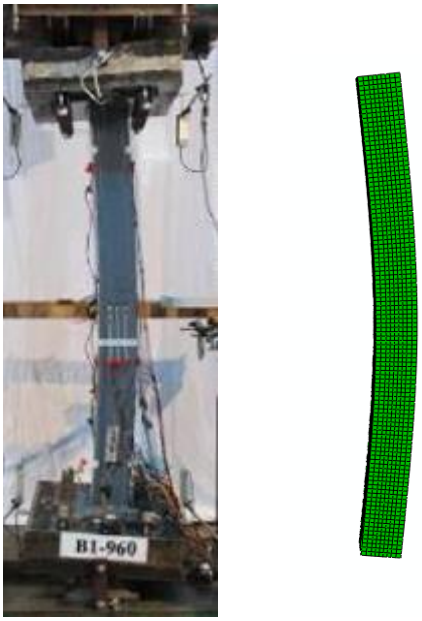

Figure 3. Comparison of the global buckling failure mode obtained from FE modelling and experiments for B142.60*13.99 [10].

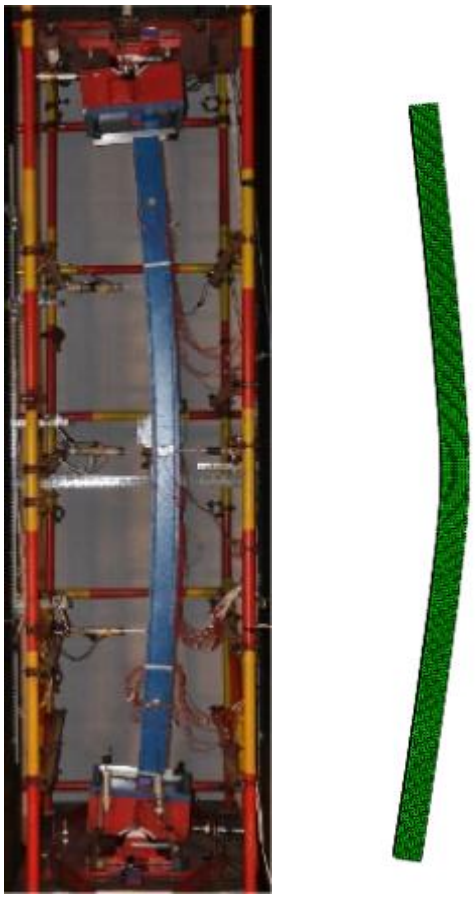

Figure 4. Comparison of the global buckling failure mode obtained from FE modelling and experiments for B120.68*12.54 [17].

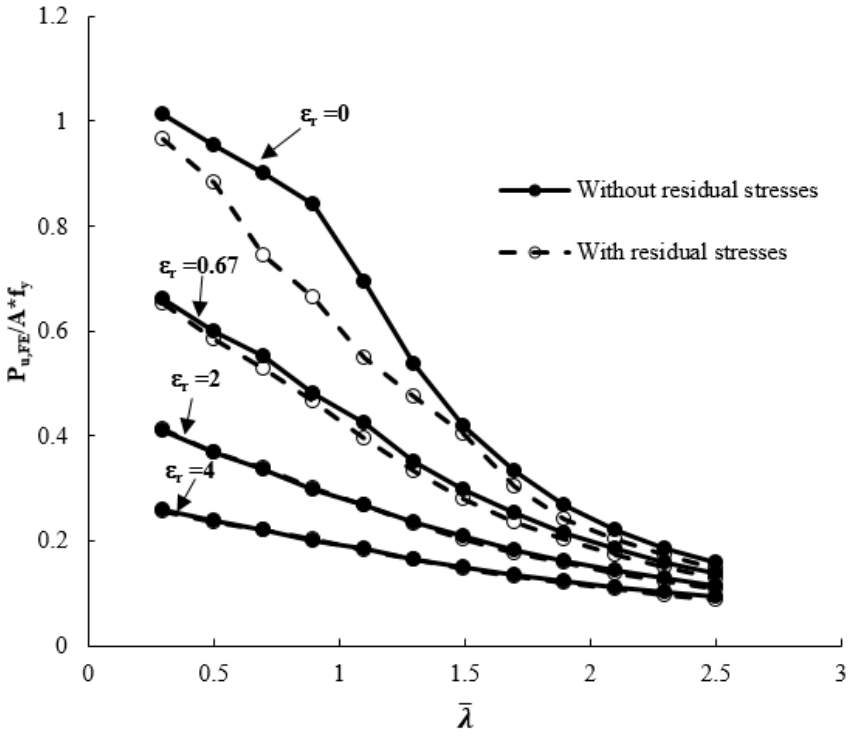

(a) S460 members

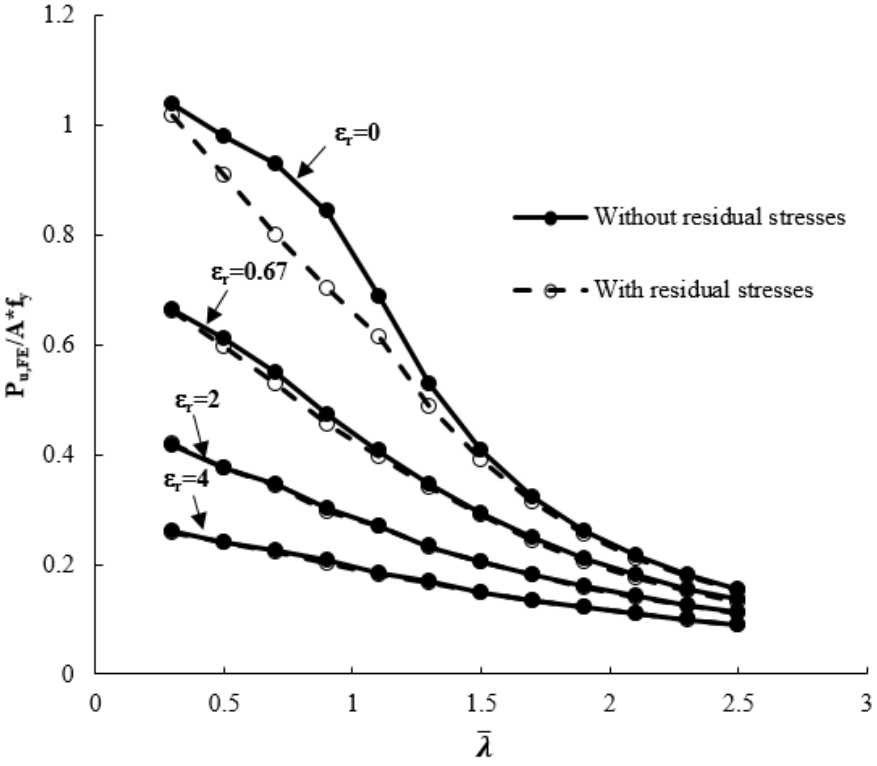

(b) S690 members

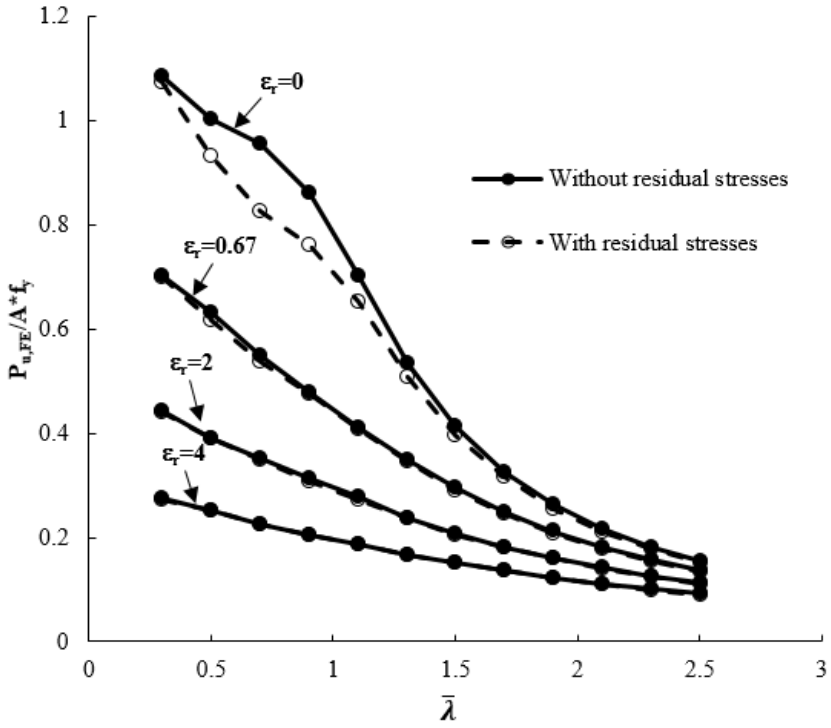

(c) S960 members

Figure 5. Comparison of the FE results obtained with and without residual stresses for S460, S690 and S960 members subject to combined compression and bending.

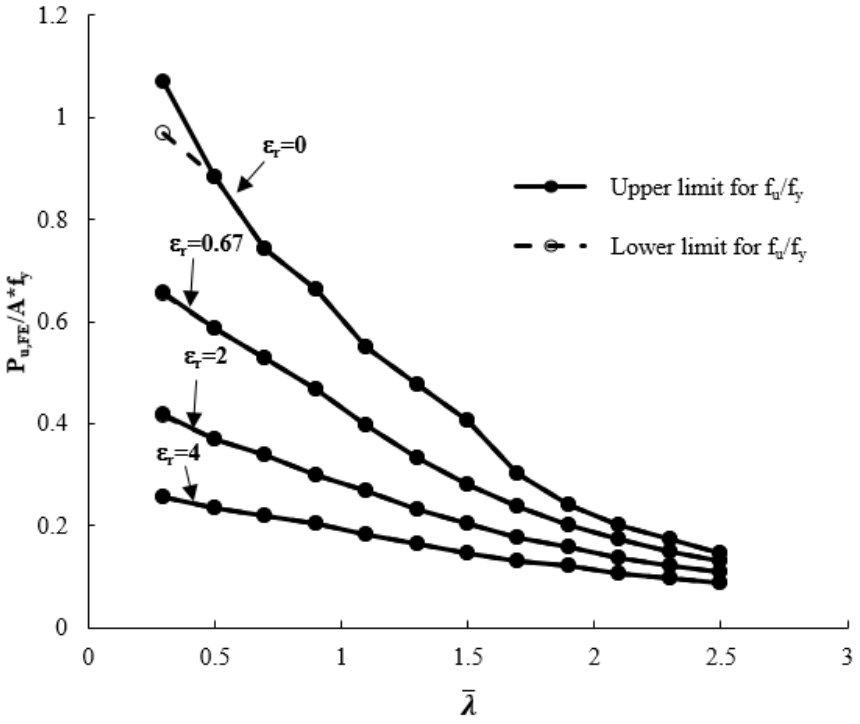

(a) S460 members

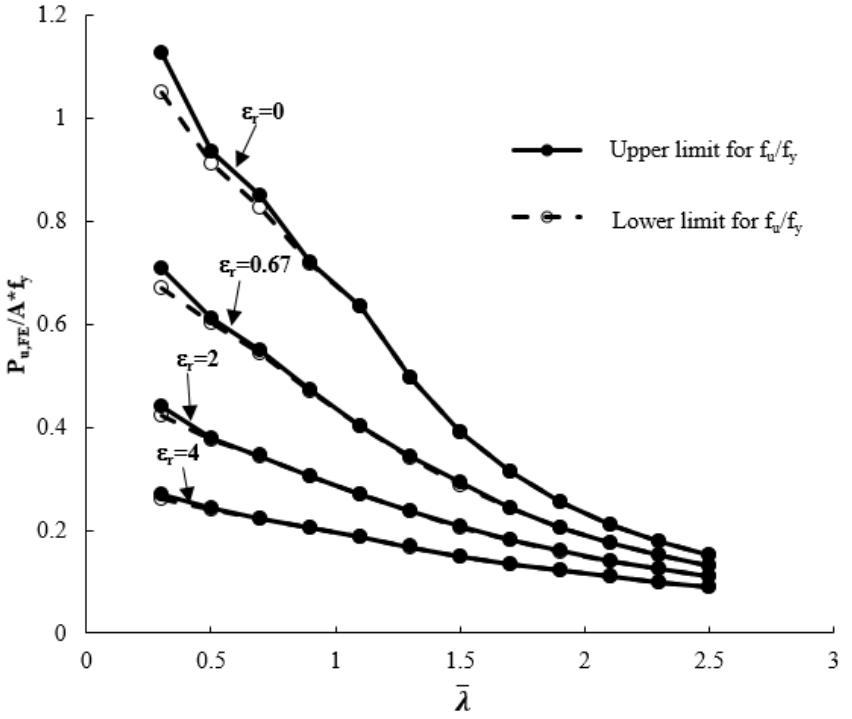

(b) S690 members

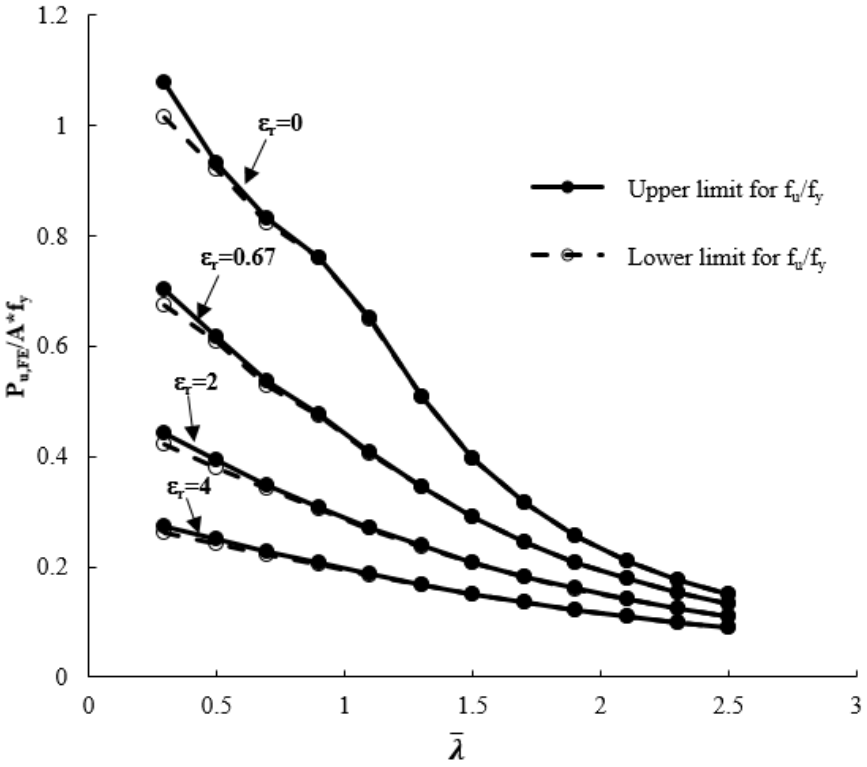

(c) S960 members

Figure 6. Comparison of the FE results obtained with different f_u/f_y ratios for S460, S690 and S960 members subject to combined compression and bending.

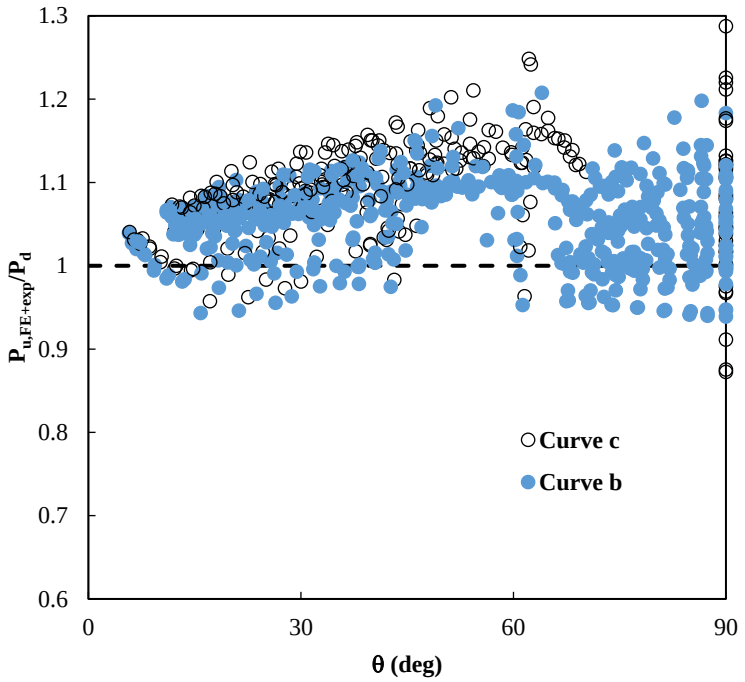
1.3
1.2
1.1
1
0.9
0.8
0.7
0.6
0
30
60
90
θ (deg)
P_u,FE+exp/P_d
Curve c
Curve b

(a)

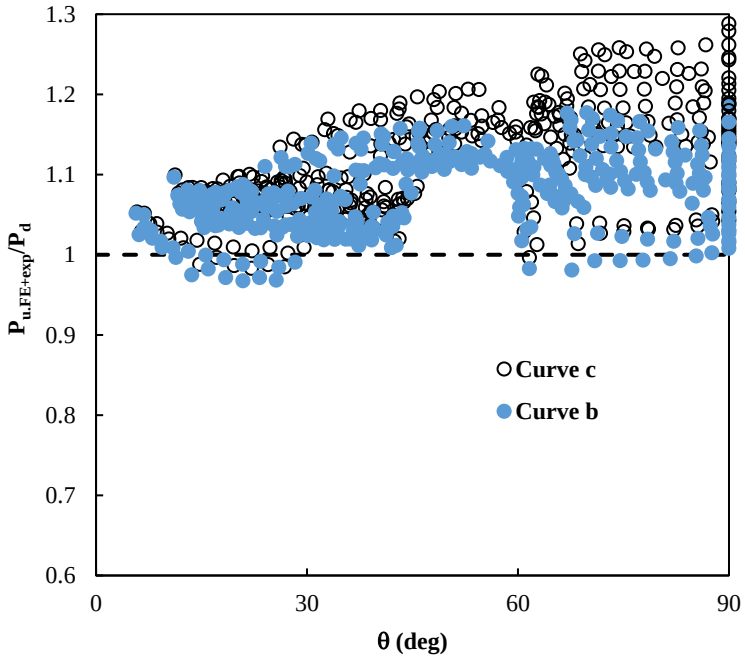
1.3
1.2
1.1
1
0.9
0.8
0.7
0.6
0
30
60
90
θ (deg)
P_u,FE+exp/P_d
Curve c
Curve b

(b)

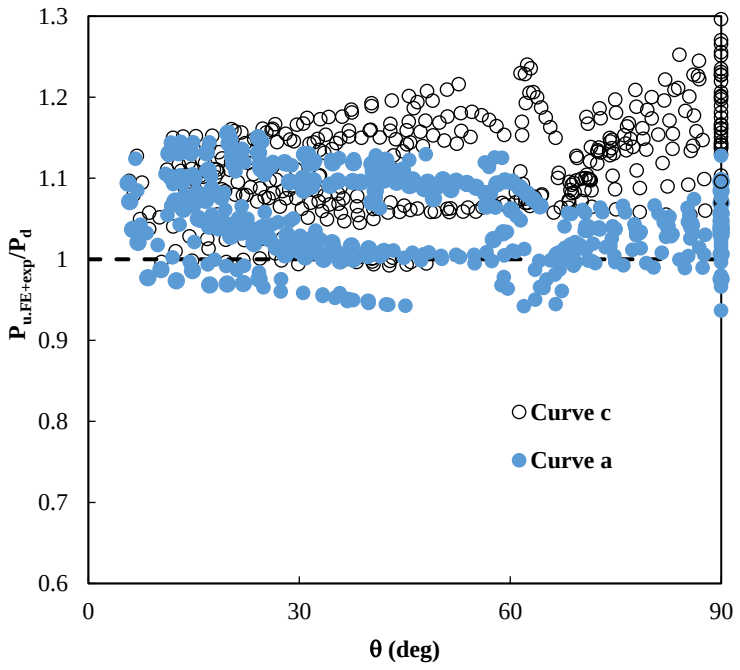

(c)

Figure 7. Comparison of P_d estimated based on Annex A in European code with the results from FE modelling and experiments reported in literature for members in steel grade of (a) S460; (b) S690 and (c) S960.

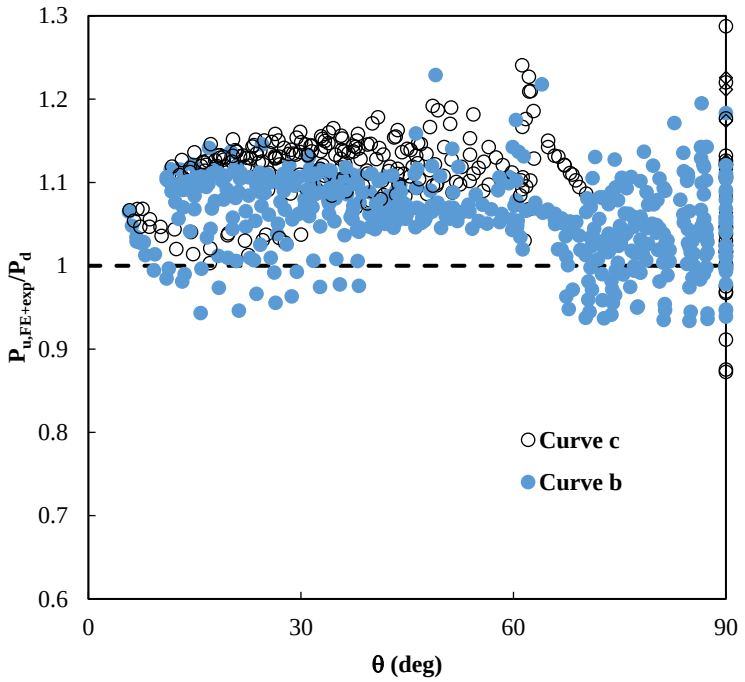
1.3
1.2
1.1
1
0.9
0.8
0.7
0.6
0
30
60
90
θ (deg)
$P_{u,FE+exp}/P_d$
Curve c
Curve b

(a)

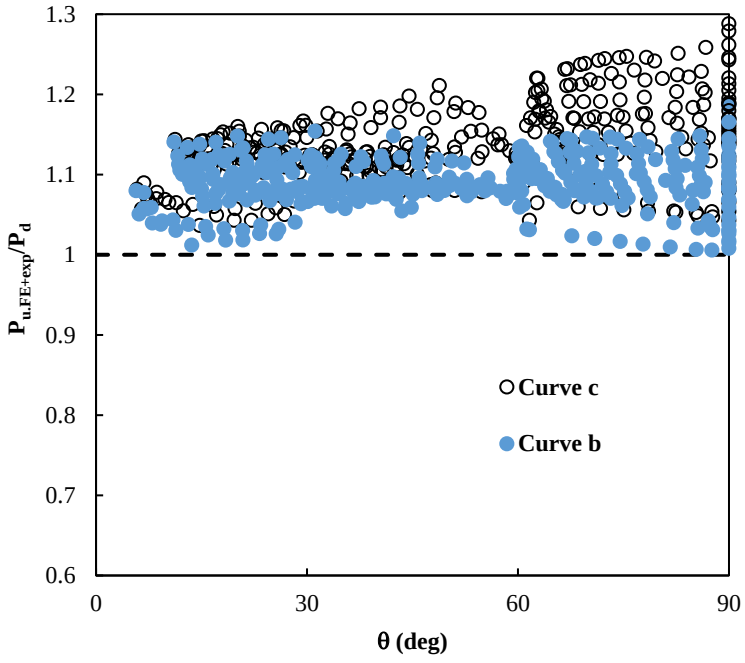
1.3
1.2
1.1
1
0.9
0.8
0.7
0.6
0
30
60
90
θ (deg)
$P_{u,FE+exp}/P_d$
Curve c
Curve b

(b)

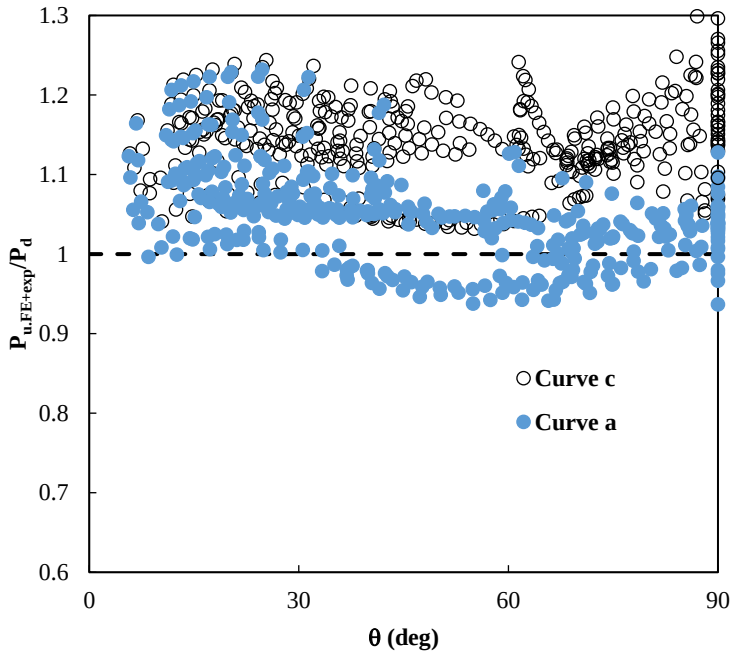

(c)

Figure 8. Comparison of P_d estimated based on Annex B in European code with the results from FE modelling and experiments reported in literature for members in steel grade of (a) S460; (b) S690 and (c) S960.

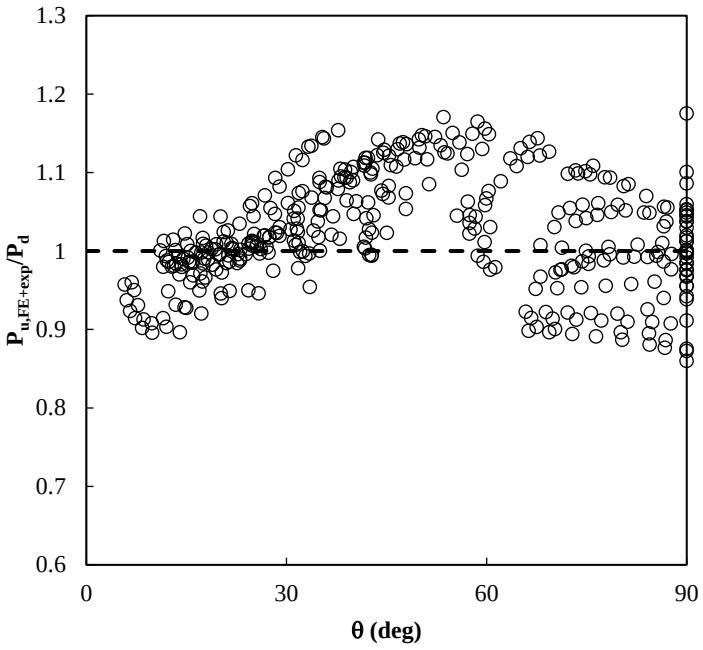
1.3
1.2
1.1
1
0.9
0.8
0.7
0.6
0
30
60
90
θ (deg)
P_u,FE+exp/P_d

(a)

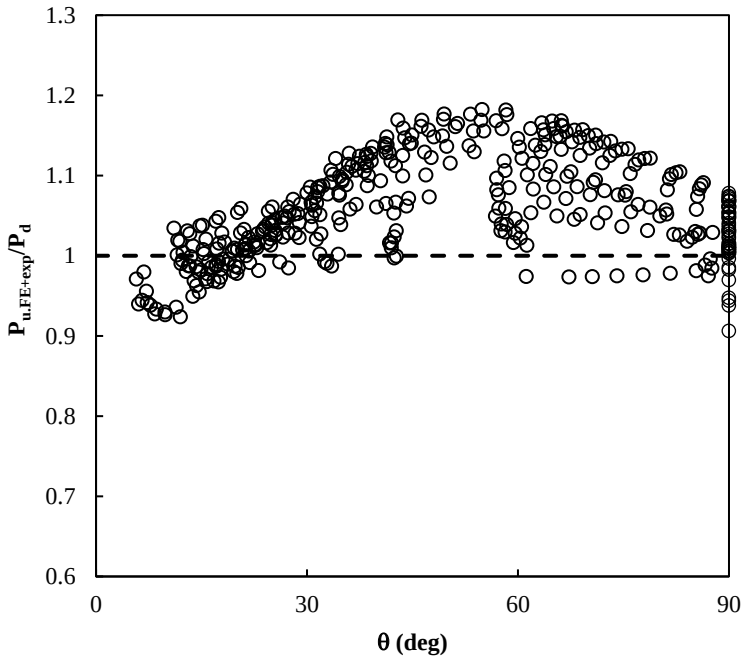
1.3
1.2
1.1
1
0.9
0.8
0.7
0.6
0
30
60
90
θ (deg)
P_u,FE+exp/P_d

(b)

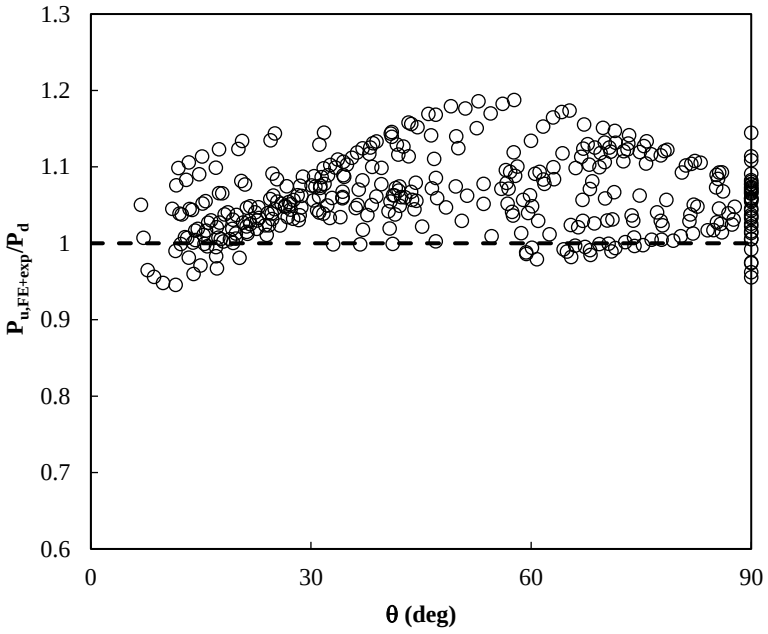

(c)

Figure 9. Comparison of P_d estimated based on AISC360 with the results from FE modelling and experiments reported in literature for members in steel grade of (a) S460; (b) S690 and (c) S960.

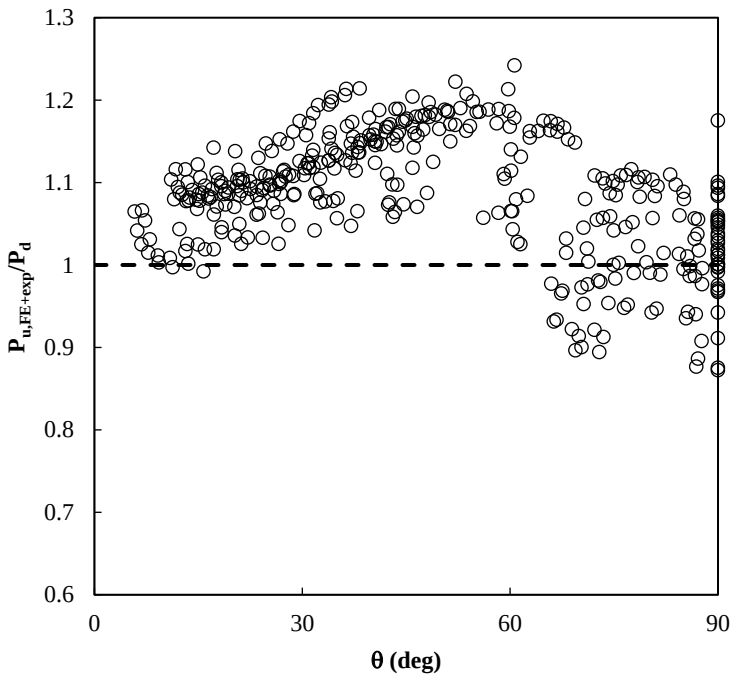
1.3
1.2
1.1
1
0.9
0.8
0.7
0.6
0
30
60
90
$P_{u,FE+exp}/P_d$
θ (deg)

(a)

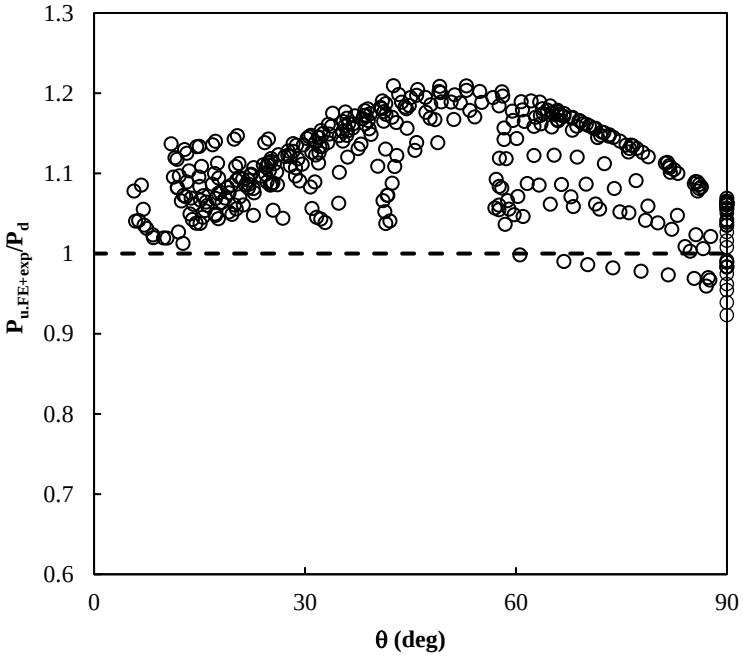
1.3
1.2
1.1
1
0.9
0.8
0.7
0.6
0
30
60
90
$P_{u,FE+exp}/P_d$
θ (deg)

(b)

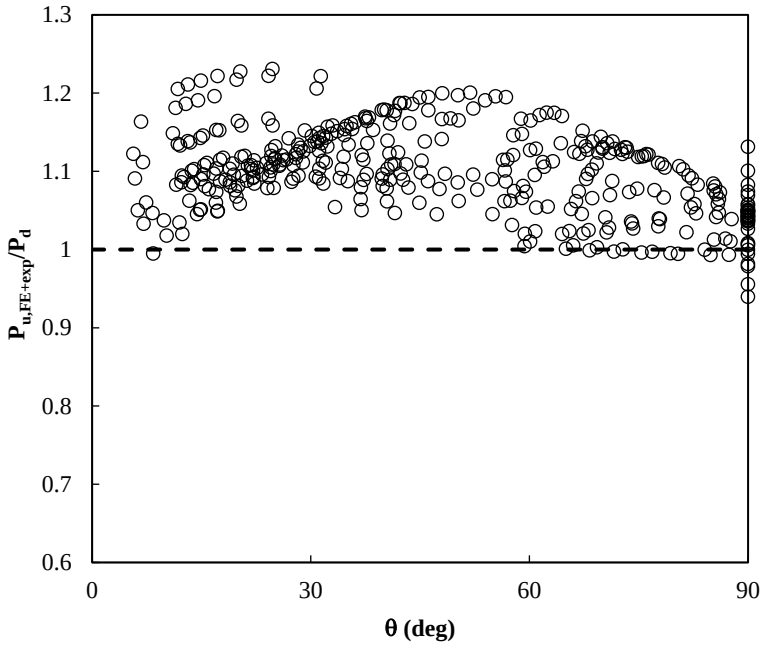

(c)

Figure 10. Comparison of P_d estimated based on AS4100 with the results from FE modelling and experiments reported in literature for members in steel grade of (a) S460; (b) S690 and (c) S960.

Table 1. Experimental data of welded HSS beam-column members.

Specimen	Yield strength f_y (MPa)	Effective length L_{eff} (mm)	Member slenderness $\bar{\lambda}$	Load eccentricity e (mm)	P_{exp} (kN)	$P_{u,FE}$ (kN)	$P_{u,FE}/P_{exp}$
B142.60*13.99 [10]	973.2	1878.6	0.77	25.88	3779.5	3852.0	1.02
B141.60*13.94 [10]	973.2	2879.8	1.19	3.13	4063.9	4084.6	1.00
B120.68*12.54 [17]	563	3392.0	1.26	48.10	861.9	871.2	1.01
B121.12*12.60 [17]	563	3391.0	1.26	79.40	642.6	674.1	1.05
B168.96*12.61 [17]	563	4009.0	1.03	28.60	2004.1	1952.1	0.97
B168.48*12.63 [17]	563	4009.0	1.04	58.80	1469.9	1453.6	0.99
B217.23*12.57 [17]	551	4072.0	0.80	44.60	2881.5	2889.1	1.00
B216.98*12.55 [17]	551	4075.0	0.80	74.00	2240.8	2267.9	1.01
B264.03*12.59 [17]	551	3583.0	0.57	30.60	4748.8	4794.7	1.01
B265.10*12.63 [17]	551	3582.0	0.57	58.80	3899.9	3979.4	1.02
B138.98*6.01 [18]	741	2090.0	0.91	10.70	1220.0	1235.2	1.01
B97.5*4.95 [19]	705	1150.0	0.56	0.90	1137.0	1157.9	1.02

B99.34*4.97 [19]	705	1950.0	0.93	2.20	926.0	905.3	0.98
B99.34*4.97 [19]	705	3450.0	1.65	-0.90	438.0	414.5	0.95
						Mean	1.00
						COV	0.02

Table 3/8

Table 2. Parameters for welded box section members for parametric studies.

Parameter	Values	Fixed value
Cross-sectional width B (mm)	120, 168, 216, 264	168
Plate thickness t (mm)	12	-
Member slenderness $\bar{\lambda}$	0.3-2.5	0.3, 0.5, 0.7, 0.9, 1.1, 1.3, 1.5, 1.7, 1.9, 2.1, 2.3, 2.5
Steel grade	S460, S690, S960	-
Global geometric imperfection/member length	1/1000	-
Eccentricity ratio (ε_r)	0-6	0, 0.67, 2, 4

Table 3. Material properties of S460, S690 and S960 HSS based on experimental measurements [10, 17-19] for parametric studies.

Steel grade	Elastic modulus (GPa)	Yield strength f_y (MPa)	Tensile strength f_u (MPa)	f_u/f_y lower limit	f_u/f_y upper limit
S460	208.5	557.0	660.0	1.20	1.56
S690	214.0	723.0	770.0	1.12	1.36
S960	208.0	973.2	1052.0	1.02	1.19

Table 4. Comparison of the global buckling resistance from FE modelling and experimental results in literature with the predicted strengths based on design methods in standards for welded S460 box section members.

Parameters	European code, Annex A		European code, Annex B		AS4100	AISC 360
	Curve c $P_{u,FE+exp}/P_d$	Curve b $P_{u,FE+exp}/P_d$	Curve c $P_{u,FE+exp}/P_d$	Curve b $P_{u,FE+exp}/P_d$	$P_{FEA}/P_{d,AS4100}$	$P_{FEA}/P_{d,AISC}$
Mean	1.09	1.05	1.11	1.06	1.09	1.03
COV	0.05	0.05	0.04	0.05	0.06	0.06

Table 5. Comparison of the global buckling resistance from FE modelling and experimental results in literature with the predicted strengths based on design methods in standards for welded S690 box section members.

Parameters	European code, Annex A		European code, Annex B		AS4100	AISC 360
	Curve c $P_{u,FE+exp}/P_d$	Curve b $P_{u,FE+exp}/P_d$	Curve c $P_{u,FE+exp}/P_d$	Curve b $P_{u,FE+exp}/P_d$	$P_{FEA}/P_{d,AS4100}$	$P_{FEA}/P_{d,AISC}$
Mean	1.11	1.08	1.14	1.10	1.11	1.06
COV	0.06	0.04	0.05	0.04	0.05	0.06

Table 6. Comparison of the global buckling resistance from FE modelling and experimental results in literature with the predicted strengths based on design methods in standards for welded S960 box section members.

Parameters	European code, Annex A		European code, Annex B		AS4100	AISC 360
	Curve c $P_{u,FE+exp}/P_d$	Curve a $P_{u,FE+exp}/P_d$	Curve c $P_{u,FE+exp}/P_d$	Curve a $P_{u,FE+exp}/P_d$	$P_{FEA}/P_{d,AS4100}$	$P_{FEA}/P_{d,AISC}$
Mean	1.12	1.05	1.14	1.05	1.10	1.06
COV	0.05	0.05	0.05	0.06	0.05	0.05

Table 7. Statistical parameters for the reliability analysis according to EN1990 for members with ε_r larger than zero.

Steel grade	ε_r	Method	n	$k_{d,n}$	b_e	V_δ	V_r	γ_{M1}
S460	ε_r=0	curve c	48	3.307	1.094	0.061	0.077	0.99
		curve b	48	3.386	1.024	0.051	0.070	1.03
	ε_r>0	Annex A, curve c	348	3.118	1.070	0.048	0.067	0.98
		Annex A, curve b	348	3.118	1.029	0.047	0.067	1.02
		Annex B, curve c	348	3.118	1.083	0.041	0.062	0.95
		Annex B, curve b	348	3.118	1.035	0.047	0.067	1.01
S690	ε_r=0	curve c	45	3.322	1.145	0.056	0.075	0.97
		curve b	45	3.322	1.071	0.041	0.0656	0.99
	ε_r>0	Annex A, curve c	344	3.119	1.122	0.057	0.075	0.93
		Annex A, curve b	344	3.119	1.079	0.046	0.067	0.95
		Annex B, curve c	344	3.119	1.139	0.039	0.062	0.91
		Annex B, curve b	344	3.119	1.089	0.027	0.056	0.93
S960	ε_r=0	curve c	40	3.354	1.184	0.056	0.072	0.96

		curve a	40	3.354	1.041	0.036	0.060	1.05
	$\varepsilon_r>0$	Annex A, curve c	342	3.119	1.125	0.053	0.070	0.97
		Annex A, curve a	342	3.119	1.043	0.048	0.066	1.05
		Annex B, curve c	342	3.119	1.147	0.046	0.064	0.96
		Annex B, curve a	342	3.119	1.054	0.051	0.068	1.04

Table 7/8

Table 8. Statistical parameters for the reliability analysis according to AISC 360.

Steel grade	ε_r	n	V_Q	V_R	ϕ	β
S460	$\varepsilon_r=0$	48	0.19	0.093	0.9	2.89
	$\varepsilon_r>0$	348	0.19	0.093	0.9	3.03
S690	$\varepsilon_r=0$	45	0.19	0.088	0.9	3.14
	$\varepsilon_r>0$	344	0.19	0.093	0.9	3.33
S960	$\varepsilon_r=0$	40	0.19	0.081	0.9	2.93
	$\varepsilon_r>0$	342	0.19	0.087	0.9	2.94